Available online at www.sciencedirect.com

ScienceDirect

Energy Procedia 61 (2014) 639 – 642

Energy Procedia

The 6th International Conference on Applied Energy – ICAE2014 #349

Comparison of Pressure Driven Electrolytic Membranes (PDEM) and Solid Electrolyte Oxygen Pumps (SEOP) for small scale oxygen production

Paolo Iora[a], Paolo Chiesa[b], Stefano Campanari[b]*

[a] University of Brescia, Dep. of Mechanical and Industrial Enginnering, Via Branze 38, 25121 Brescia, Italy
[b] Politecnico di Milano, Department of Energy, via Lambruschini 4, 20156 Milano, Italy

Abstract

This work evaluates the thermodynamic performances of two oxygen separation technologies, Pressure Driven Electrolytic Membranes (PDEM) and Solid Electrolyte Oxygen Pumps (SEOP), focusing on the application to small scale oxygen production. We show that PDEM systems operated with a specific flux of 5 liters of oxygen per minute per square meter of active membrane surface (5 L_{O2}/min-m^2) can reach an energy consumption as low as 0.39 kWh/kg_{O2}. In the same conditions with a SEOP, the optimized energy consumptions are 0.52 and 0.49 kWh/kg_{O2} respectively for atmospheric and pressurized configurations.

Peer-review under responsibility of the Organizing Committee of ICAE2014

Keywords: Oxygen production, Electrolytic membranes, Electrolyte oxygen pumps, PDEM, SEOP

1. Introduction

Distributed oxygen generation can be a suitable solution in several industrial sectors as well as for medical treatments [1]. Presently, most of the small scale oxygen generators on the market are based on PSA (pressure swing adsorption) or VSA (vacuum swing adsorption) technologies or hybrid solutions between the former ones, which exploit the greater affinity for N_2 than for O_2 of specific adsorbent materials such as the zeolites. Although they represent a well-established technology, their efficiencies are considerably lower than those of large scale cryogenic plants, resulting in higher variable costs for the oxygen yield. For instance, while the specific consumption for large-scale cryogenic plants can reach 0.2 kWh/kg_{O2}, PSA and VSA technologies show energy consumption in the range 0.7–1.0 kWh/kg_{O2} for product rates around 100 kg_{O2} per day [2]. Aiming to achieve an efficiency improvement at the lower end of the output rate scale, new technologies have emerged in the last years, especially based on chemical looping concept and membrane separation [3,4]. This paper compares the thermodynamic performances of two of these innovative technologies, the oxygen Pressure Driven Electrolytic Membranes (PDEM) and Solid Electrolyte Oxygen Pumps (SEOP), individuating the system layout that allows oxygen separation from air.

2. Pressure driven electrolytic membranes (PDEM)

* Corresponding author. Tel.: +39-0223993862; E-mail: stefano.campanari@polimi.it

Peer-review under responsibility of the Organizing Committee of ICAE2014
doi:10.1016/j.egypro.2014.11.1187

Within PDEM systems, selective oxygen transport across an electrolytic membrane is the result of a driving force provided by a difference of partial pressure on the two sides of the membrane. Oxygen transport across the membrane relies on five different steps. First (i) O_2 transfers from feed stream to the membrane surface, then (ii) adsorption and dissociation of oxygen within the membrane takes place; then (iii) oxygen is transported through the membrane. Final steps are (iv) oxygen association and desorption and (v) mass transfer to the permeate gas stream. Assuming that surface kinetics occurs at higher rates than bulk transport (that is true for a thick membrane), O_2 permeation can be expressed as:

$$\varphi = k \cdot \ln\left(p_{feed} / p_{perm}\right) \quad (1)$$

where p_{feed} and p_{perm} are the O_2 partial pressure on the feed side (where compressed air is supplied) and on the separated oxygen side respectively. As membrane thickness reduces, bulk transport resistance decreases so that surface reaction resistance is no more negligible and flux is not fully governed by Eq. (1). Nevertheless, we assumed for simplicity that Eq. (1) holds also for thin membranes, evaluating the coefficient k from experimental data on a 30 μm thick LSCF asymmetric supported membrane [5], where it can be assumed $6 \cdot 10^{-6}$ kmol$\cdot$s$^{-1}\cdot$m^{-2} when the membrane temperature is kept in the range of 850-900 °C.

Figure 1 shows the proposed PDEM system layout. Ambient air is compressed (stream 2) and preheated in the recuperator (stream 3). A final heating at 850°C is necessary to operate the membrane at the correct temperature and to keep a proper temperature difference on the hot end of the recuperator. Heating is provided by an electric heater (stream 3 to 4). Air is then fed to the PDEM (stream 4) that accomplishes the partial separation of oxygen. Heat from both the depleted air (stream 6) and the separated oxygen (stream 5) are recovered within the recuperator. Finally the depleted air is expanded (stream 7) to provide part of the mechanical power necessary for the air compression. The remaining power must be supplied by an electric motor.

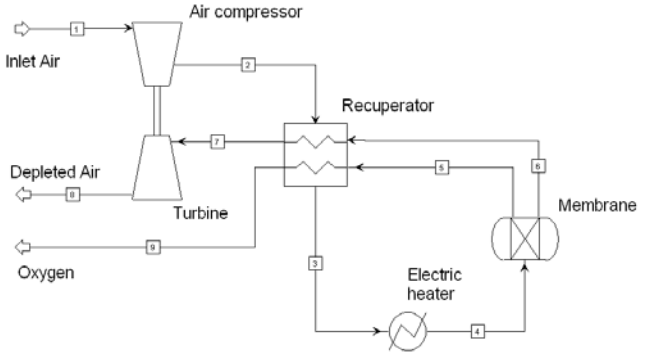

Figure 1. PDEM system layout.

Compressor isentropic efficiency	0.75
Turbine isentropic efficiency	0.80
Minimum ΔT in the recuperator	50 °C
Overall system pressure losses	0.2 bar
PDEM active area	1 m^2
PDEM back-pressure	1.05 bar

Table 1. Calculation assumptions for the system layout shown in Fig. 1.

Energy and mass balances of the plant layout have been simulated with Aspen Plus. The air compressor, turbine, recuperator and electric heater are modelled as 0-D components using the software model library, with the calculation assumptions reported in Tab. 1. Regarding the PDEM, we assumed a membrane active area of 1 m^2 and we developed a 1-D model in which the membrane is divided into 50 intervals along the air flow path. By locally applying Eq. (1) it is possible to determine in each interval the permeated O_2 flux. For a fixed membrane area and O_2 back pressure (assumed at 1 bar), the overall permeated oxygen flow is then determined by the air flow rate and pressure (stream 4 in Fig. 1).

Results of the simulation are presented in Fig. 2 in case of oxygen flux of 5 l/min-m^2. The overall system specific consumption for oxygen separation (kWh_{el} per kg of separated oxygen) is plotted as a function of the air pressure, together with the required air flow. Trend of curves can be explained as follows. As feed side pressure increases the O_2 fraction removed from air increases thanks to the higher difference in O_2 partial pressure between the feed and the permeate side: therefore, keeping a fixed O_2 flow rate, the required air flow rate reduces. On the other hand, the turbocharger work input increases with air pressure. Globally, the opposite trend of the two factors brings to an optimum pressure of 18 bar where the overall system consumption is minimized at 0.39 kWh/kg_{O2} , with the energy balances given in Tab. 2. Although

the simulation is carried out with several simplified assumptions, the result is very interesting since the consumption is about one third of the typical consumption of commercial oxygen supplying devices of the same size.

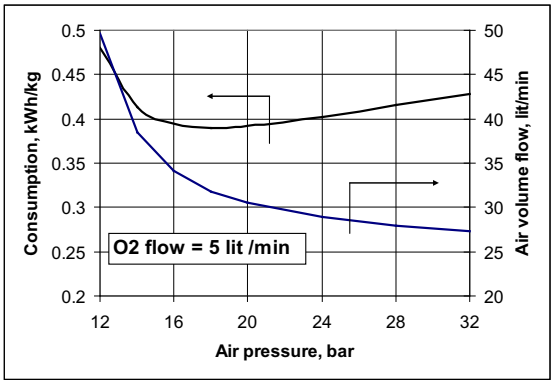

Figure 2. Overall system specific consumption (left axis) and air flow rate (right) as function of the air pressure in case of O_2 flux of 5 L_{O2}/min-m^2.

Energy balance	[W]
Air compressor power consumption	330
Turbine power output	210
Net shaft power required for air compression	120
Electric Heater consumption	38
Recuperator thermal duty	211

Table 2. Energy balance of the system shown in Fig. 1 in case of O_2 flux of 5 L_{O2}/min-m^2 at optimized air feed pressure (18 bar).

Similar results are obtained with O_2 production of 3 and 7 L/min, yielding a min. energy consumption of 0.38 kWh/kgO_2 at 15 bar or 0.42 kWh/kgO_2 at 24 bar respectively. It can be concluded that for a fixed membrane area the increase of oxygen production implies an increase of both the optimized air pressure and overall energy consumption.

3. Solid electrolyte oxygen pumps (SEOP)

SEOP systems are based on solid oxygen ion conductors which are able to permeate and compress oxygen when a voltage is applied. They can be adopted to arrange ‘‘electrically driven’’ oxygen separation systems also referred to as solid electrolyte oxygen pumps (SEOP). The ideal voltage V_{id} necessary to drive the separation process from air is given by:

$$V_{id} = RT/4F \times \ln(p_{perm}/p_{feed}) \qquad (2)$$

where p_{feed} is the O_2 partial pressure in the air, p_{perm} is the pressure of the separated oxygen, F the Faraday constant, T the temperature and R the universal gas constant. We consider two different cases operating at atmospheric pressure or – with a more complex layout – using a turbocharger (compressor + turbine) to supply pressurized air to the SEOP. The layout necessary to operate the SEOP in atmospheric mode is shown Fig. 3.

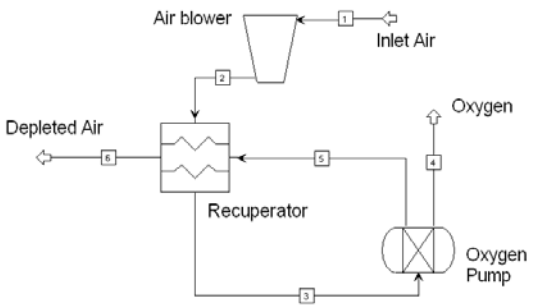

Figure 3. System layout for atmospheric SEOP.

Blower / compressor isentropic efficiency	0.75
Turbine isentropic efficiency (only for pressurized SEOP)	0.80
Minimum ΔT in the recuperator	100 °C
SEOP inlet temperature	750°C
SEOP outlet temperature	850°C
Overall system pressure losses	0.2 bar
Active area of the SEOP cell	1 m^2
Cell overall resistance R [6]	0.73 Ω/cm^2
O_2 back pressure of the SEOP	1.05 bar

Table 3. Calculation assumptions in case of atmospheric SEOP.

A blower supplies ambient air (stream 1) to the recuperator where it is heated to 750 °C before feeding the SEOP at ambient pressure, separating part of the oxygen (stream 4). Heat from the depleted air is recovered in the recuperator (stream 5). Calculation assumptions are listed in Tab.3. Simulations are

carried out for a produced O_2 flow rate (stream 4) of 3, 5 and 7 L/min. In each case the air flow rate was optimized to minimize the overall system consumption. Results of the simulations are reported in Tab. 4, where the current density is referred to the active area of the SEOP, the ideal voltage is defined according to Eq. 2 and the polarization voltage is given by $\Delta V_{pol}=R\times i$. The total operating voltage is $V_{OP} = V_{id} + \Delta V_{pol}$. Adding the blower consumption we obtain a system consumption of 0.521 kWh/kg_{O2} for an O_2 production of 5 L/min. Results are strongly influenced by the assumed value of cell resistance; however they show higher consumptions with respect to the PDEM, although with a simpler plant layout.

O_2 yield, L/min	Air flow L/min	Current density A/m^2	Ideal voltage V	ΔV_{pol} V	V_{OP} V	$P_{el,\ SEOP}$ W	P_{blower} W	Total consumption kWh_{el}/kg_{O2}
3	28.4	816	0.0403	0.0596	0.0998	81.5	12.4	0.385
5	42.6	1360	0.0424	0.0993	0.1417	192.8	18.6	0.521
7	56.7	1905	0.0442	0.1390	0.1832	348.9	24.7	0.657

Table 4. Simulation results in case of atmospheric SEOP.

In the pressurized case it is possible to employ a turbocharger (compressor + turbine) in order to supply pressurized air to the SEOP; the compressor is partially driven by a turbine which expands the recuperator outlet stream, with an electric motor providing the remaining part of the required power. Differently from the PDEM case, the electric heater is not necessary as the heat rejected by the SEOP is sufficient to heat up the outlet streams keeping the ΔT_{min} of 100°C in the recuperator. Table 5 reports the results of the simulations in case of O_2 yield of 5 L/min, as function of the operating pressure. The air flow rate (second column) was optimized to minimize the system consumption.

SEOP pressure bar	Optimized air flow, L/min	SEOP Power, W	Turbocharger Power, W	System Consumption, kWh_{el}/kg_{O2}
2	30.4	181.6	24.7	0.508
4	28.4	159.8	39.5	0.491
6	28.4	147.0	52.8	0.492
8	28.4	138.0	63.6	0.496

Table 5. Results of the pressurized SEOP case, oxygen production 5 L/min.

An increase of the air feed pressure reduces SEOP power consumption while it increases the power consumed by the turbocharger, yielding an optimum pressure at 4 bar. Similar results are obtained at 3 and 7 L_{O2}/min, where the min. energy consumption at 4 bar is 0.357 and 0.624 kWh/kgO_2 respectively.

4. Conclusions

In this paper, we evaluate the thermodynamic performances of two oxygen separation technologies, Pressure Driven Electrolytic Membranes (PDEM) and Solid Electrolyte Oxygen Pumps (SEOP), focusing on the application to small scale oxygen production. The analysis of a system based on PDEM with active area of 1 m^2 shows that for a target production of 5 L/min of O_2, the system consumes about 0.39 kWh/kg_{O2} with air fed to the membrane at 18 bar. Higher O_2 flux can be obtained at increased air pressure and slightly higher energy consumption, so that the optimum value of O_2 flux should be determined by means of an overall system costs analysis. In case of the SEOP system, with an atmospheric configuration we obtain a consumption of 0.385 to 0.657 kWh/kg_{O2} for oxygen production rate ranging from 3 to 7 L/min. A 5-7% reduction in system consumption can be obtained by adopting a pressurized configuration. Results are nevertheless strongly dependent on the assumed value of SEOP cell resistance.

References

[1] M.J. Kirschner, Oxygen, Ullmann's Encyclopedia of Industrial Chemistry, Wiley-VCH Verlag GmbH & Co. KGaA, 2000.
[2] Iora P, Chiesa P. High efficiency process for the production of pure oxygen based on the SOFC–SOEC technology. J Power Sources 2009; 190:408–416.
[3] Iora P, Thaer M, Chiesa P, Brandon NP. A one dimensional solid oxide electrolyzer-fuel cell stack model and its application to the analysis of a high efficiency system for oxygen production. Chemical Engineering Science 2012; 80:293-305.
[4] Dyer PN, Richards RE, Russek SL, Taylor DM. Ion transport membrane technology for oxygen separation and syngas production. Solid State Ionics 2000;134:21–33.
[5] Serra J.M., Garcia-Fayos J., Baumann S. Schulze-Küppers F., Meulenberg W.A. Oxygen permeation through tape-cast asymmetric all-$La_{0.6}Sr_{0.4}Co_{0.2}Fe_{0.8}O_{3-\delta}$ membranes. Journal ofMembraneScience 2013, 447:297–305
[6] Laguna-Bercero MA, Kilner JA, Skinner SJ. Development of oxygen electrodes for reversible solid oxide fuel cells with scandia stabilized zirconia electrolytes. Solid State Ionics 192 (2011) 501–504.